ELSEVIER

Journal of Physics and Chemistry of Solids 63 (2002) 827–832

JOURNAL OF PHYSICS AND CHEMISTRY OF SOLIDS

www.elsevier.com/locate/jpcs

Thermoelectric properties of tin clathrates under hydrostatic pressure

F. Chen[a,*], K.L. Stokes[a], G.S. Nolas[b]

[a]*Advanced Material Research Institute, University of New Orleans, New Orleans, LA 70148, USA*
[b]*Department of Physics, University of South Florida, Tampa, FL 33620, USA*

Received 16 July 2001; accepted 24 September 2001

Abstract

We report the temperature dependence of electrical resistance (R) and thermopower (S) of clathrate Cs_8Sn_{44} under high pressure up to 1.2 GPa. We observe a reversible gap widening, prominent relaxation effect of R, irreversible increase of $|S|$ under high pressure. We also find that the power factor $S^2\sigma$ (σ: electrical conductivity) reaches a maximum at pressure of 0.3 GPa. Comparison of the experimental results with band structure calculations suggests that the intrinsic vacancy in the clathrate structure of Cs_8Sn_{44} plays an important role in transport properties under high pressure. Measurements on $Cs_8Zn_4Sn_{42}$, a clathrate which has defects other than vacancies, are compared with Cs_8Sn_{44}. The results indicate that replacing Sn by Zn has similar effect as the intrinsic vacancy on S.

PACS: 72.20.P; 71.20; 84.60.R; 07.35

Keywords: C. High pressure; D. Electronic structure; D. Defects

1. Introduction

The use of high pressure in material science can be a powerful tool to synthesize novel materials, to simulate hypothetical chemical substitution, to uncover underlying systematics and to compare and give more hints for band structure theories [1,2]. In this paper, we study the thermoelectric properties of semiconducting clathrate compounds as a function of both hydrostatic pressure and temperature.

Compounds of group IV elements that form into clathrate-type structures possess high Seebeck coefficient and electrical conductivity while their thermal conductivity values are low [3]. This has stimulated much research interest in these compounds as potential materials for thermoelectric applications [4–7]. Interestingly, several clathrates were found to be superconductors [8]. Transport properties [9], compressibility, phase transformations [10,11] and band structure calculations [12] were studied for Si clathrates under high pressure. Thermopower at room temperature for Ge clathrates were reported to increase almost twice under non-hydrostatic pressure up to 7 GPa [13]. Transport properties of Sn clathrates were reported before [3,14]. Among these compounds, Cs_8Sn_{44} was indicated to have multi-band conduction, with a very small activation energy near room temperature. Theoretical calculations of the band structure of clathrate Sn_{46} show that the energy gap closes under pressure [15]. If Cs_8Sn_{44} behaves similarly, we expect this very small gap to change from positive to negative under high pressure and introduce a transition from semiconductor to semi-metal. Here, we report transport measurements of Cs_8Sn_{44} under high pressure and the observation of an increase in the band gap with increasing pressure. We also compared calculated band structure of this sample by Dong et al. [15] and propose that the location of the vacancy sites changes after application of high pressure. To compare the result, we also measured the sample $Cs_8Zn_4Sn_{42}$ and observed a similar irreversible effect on S as well as a lack of a relaxation effect on R after change of pressure. The results indicate a generalized defect picture in $Cs_8A_nSn_{46-n}$, where A = Zn or vacancy.

2. Experimental setup

The sample synthesis and preparation are described in

* Corresponding author. Fax: +1-504-280-3185.
E-mail address: fchen@uno.edu (F. Chen).

0022-3697/02/$ - see front matter
PII: S0022-3697(01)00236-0

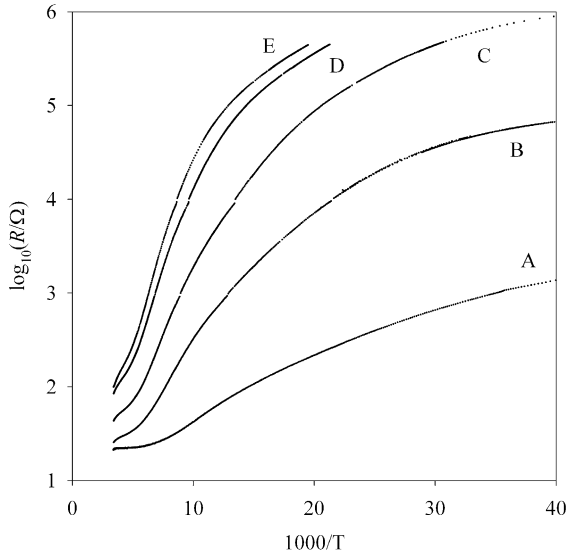

Fig. 1. Resistance versus temperature for Cs_8Sn_{44} under different pressure. The pressure in GPa for each curve is A: 0.0, B: 0.30, C: 0.60, D: 0.90, E: 1.20, respectively.

detail elsewhere [14,16]. Briefly, the samples are made using powder metallurgy techniques. Stoichiometric amounts of the the constituent material are reacted at high temperatures (550 °C) in an inert atmosphere. The resulting crystals are ground into a fine powder and the structural properties are measured by X-ray and neutron diffraction. For transport measurements, the powders are hot pressed inside a graphite die at 380 °C and approximately 0.15 GPa for 2.5 h in an argon atmosphere. This pressure is much lower than the maximum pressure we applied to the samples when doing the transport measurements.

The hydrostatic pressure was generated inside a Teflon cup housed in a Be–Cu high pressure clamp [17]. The 3M Fluorinert was used as the pressure medium in order to get highly *hydrostatic* pressure. The pressure was calculated by the force over area at room temperature. Our previous experiments used superconducting Pb as a manometer to measure pressure near liquid helium temperature and demonstrated that the pressure obtained using this method is within 10% throughout the temperature range 4–300 K [18,19].

Table 1
The energy gap E_1 at higher temperature and E_2 at lower temperature for Cs_8Sn_{42} at different pressure

P (GPa)	0.0	0.30	0.60	0.90	1.20
E_1 (meV)	1.2	14	24	38	57
E_2 (meV)	17	41	59	81	86
T^*(K)	101	138	214	407	550
k_BT^* (meV)	9	12	18	35	47

The resistance was measured using dc four-probe method. The resistivity was calculated using the geometrical factors at ambient pressure. The Seebeck coefficient under high pressure was measured using a very low frequency ac two-heater method [19,20]. Two surface mount resistors were driven by sinusoid currents that differ in phase by $\pi/2$. The amplitude of the currents can be adjusted to minimize the ac component of the base temperature fluctuation ($\tilde{T}$). The ratio ($\delta T/\tilde{T}$) of ac temperature gradient (δT) versus the base temperature fluctuation is typically greater than 10. In the previous paper, we showed that an important error in ac Seebeck measurement is [20]

$$S_{\text{measured}} - S(\tilde{T}) = S'(\tilde{T})\frac{\tilde{T}\Delta T}{\delta T}, \tag{1}$$

where S_{measured} is the measured experimental quantity for the relative thermopower, $S(\bar{T})$ is the thermopower for the temperature $\bar{T}$, $\bar{T}$ is the time average of the base temperature of the sample, while $S'(\tilde{T})$ is the derivative of $S(T)$ at the temperature $\tilde{T}$. Thus we are confident that our ac measurement gives the correct and precise S. Two pairs of T-type thermocouples were attached to the sample directly using pure indium and three independent signals were measured simultaneously to solve for the base temperature, temperature gradient and the Seebeck coefficient. The copper leads of the T-type thermocouples were calibrated relative to Pb using data from Roberts [21]. Our Teflon cell is about 3 mm in diameter and 7 mm long, thus the sample size can be much larger than that could be measured in an anvil cell and ensures precise result together with other careful considerations. Even with the surrounding of fairly good thermally conducting pressure medium, the measured Seebeck coefficient is in good agreement with that was measured outside of the pressure cell. The small pressure effect on thermocouples were also considered and corrected.

3. Results

Fig. 1 shows resistance R versus temperature T for Cs_8Sn_{44} taken at ambient pressure, 0.30, 0.60, 0.90, and 1.20 GPa. The curve for each pressure is labeled as A, B, C, D and E, respectively. We can see the sample shows semiconductor-like behavior except a very small temperature region near 295 K showing positive dR/dT at ambient pressure. After the sample is pressurized, with the gaps increasing, dR/dT becomes negative.

Fig. 1 also shows that the curves can be roughly divided into three characteristic regimes. For curve A, for values of $1000/T$ between 3.6 and 6.0 K^{-1} ($167 < T < 278$ K), it is semiconductor with a well defined energy gap E_1 as small as 1.2 meV at ambient pressure. For $1000/T$ between 7.5 and 13 K^{-1} ($77 < T < 133$ K), the curve can fit assuming a second energy gap $E_2 \approx 16.7$ meV at ambient pressure. One trend is thus obvious in Fig. 1: both E_1 and E_2 increase with pressure. Although we have not identified the precise

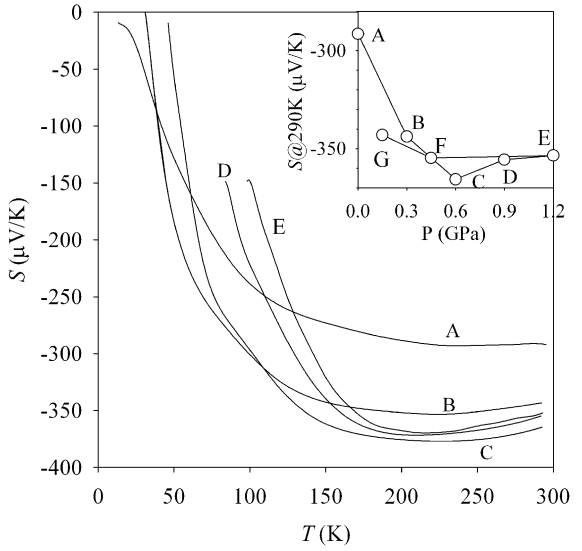

Fig. 2. Seebeck coefficient versus temperature for Cs_8Sn_{44} under different pressure. Inset: Seebeck coefficient at $T = 290$ K versus pressure. The pressure in GPa for each curve/point is A: 0.0, B: 0.30, C: 0.60, D: 0.90, E: 1.20, F: 0.45, G: 0.15, respectively, the sequence of applying pressure is A, B, C, D, E, F and then G.

nature of these two energy gaps, we can still conclude that the pressure increases the narrow band gap(s) of Cs_8Sn_{44}. Table 1 lists E_1 and E_2 for different pressures. While both E_1 and E_2 increase linearly with pressure, E_1 increases more rapidly with pressure, that is, $\partial E_1/\partial P > \partial E_2/\partial P$.

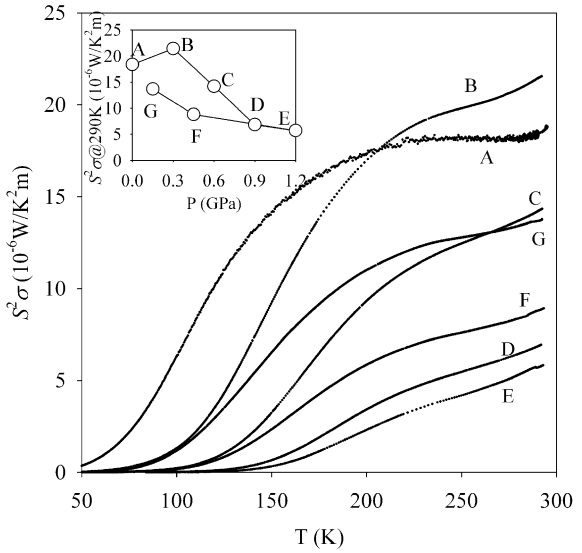

Fig. 3. Power factor $S^2\sigma$ versus temperature for Cs_8Sn_{44} under different pressure. Inset: Power factor at $T = 290$ K versus pressure. The pressure in GPa for each curve/point is A: 0.0, B: 0.30, C: 0.60, D: 0.90, E: 1.20, F: 0.45, G: 0.15, respectively, the sequence of applying pressure is A, B, C, D, E, F and then G.

Fig. 2 shows the Seebeck coefficient S versus T for ambient pressure, 0.30, 0.60, 0.90 and 1.20 GPa. The curve for each pressure is again labeled as A,B,C,D and E, respectively. For curve A, we notice that S above 200 K is very flat, which resembles the behavior for some semiconductors, e.g. ZnSb [22]. Below this temperature, the Seebeck coefficient has a strong temperature dependence. For the purpose of our analysis, we assume a relationship between the Seebeck coefficient and the Fermi energy, k_BT^*, [22,23]

$$S = \frac{k_B}{e}\left[\left(r + \frac{5}{2}\right) - \frac{T^*}{T}\right], \tag{2}$$

where k_B is the Boltzmann constant, e is the electron charge in our case, and r is an electronic scattering parameter equal to $-1/2$ for acoustic phonon scattering. The characteristic temperature T^* describes the degree of temperature dependence. Other curves in Fig. 2 show similar trend, while the T^* increases monotonically with pressure, the Seebeck coefficient at room temperature increases drastically upon application of pressure, reaches a maximum in absolute value at $P = 0.60$ GPa, and drops slightly after that, as shown in the inset of Fig. 2. We are cautious not to draw any conclusion from this apparent decrease in Seebeck coefficient, but it is obvious that S does not continue to dramatically increase when P is above 0.60 GPa.

We plotted the power factor ($S^2\sigma$) versus temperature for different pressure in Fig. 3. The electrical conductivity σ here was calculated using the geometrical factors at ambient pressure and contributes a small and negligible systematic error to the power factor. The inset of Fig. 3 shows the power factor at temperature of 290 K against pressure. In Table 2 we listed S and the power factor for different pressures at a temperature of 290 K when pressure was increased. We have not been able to measure thermal conductivity (κ) under high pressure yet, but from the result of power factor, an increase of figure of merit $Z = S^2\sigma/\kappa$ under high pressure for Cs_8Sn_{44} is very optimistic. Since the maximum power factor was achieved at pressure as low as 0.3 GPa, with some tradeoff, it is possible to get higher Z under high pressure for real thermoelectric device.

4. Discussion

It would be interesting to discuss the physical meaning of T^*. For semiconductors, Eq. (2) is valid in the nondegenerate approximation. Nevertheless, in most cases, the scattering parameter r in Eq. (2) is not temperature dependent and remains constant for a given electron scattering mechanism. The T^*/T term is, in general, more temperature dependent, and the value k_BT^* is the chemical potential, which in general is not a constant either. However, since the curve of our S resembles those of semiconductors like ZnSb [22] very much, this treatment of T^* as a constant is reasonable and gives us sufficient information about the electronic structure. In our case, this T^* reflects the change induced

Table 2
The Seebeck coefficient S and the power factor $S^2\sigma$ at 290 K for Cs_8Sn_{44} under high pressure

P (GPa)	0.0	0.30	0.60	0.90	1.20
S (μV/K)	−291	−344	−366	−356	−353
$S^2\sigma$ (10^{-6}W/K^2 m)	18.35	21.43	14.19	6.85	5.71

by pressure clearly. From Table 1, it turns out k_BT^* agrees well with E_1 at all pressures except that of ambient pressure. It is natural to attribute this deviation to the broken approximation required for Eq. (2); that is, the scattering parameter r and the Fermi energy (and hence, T^*) would not be constant with temperature for very small energy gaps E_1. Furthermore, the values thus extracted would help to compare different theoretical models.

As for E_1 and E_2, since the low temperature gap E_2 is larger than the higher temperature gap E_1, both gaps are likely to be intrinsic gaps rather than from activation of impurities. The agreement of k_BT^* with E_1 also serves as an evidence that the gap is not likely to be impurity gap.

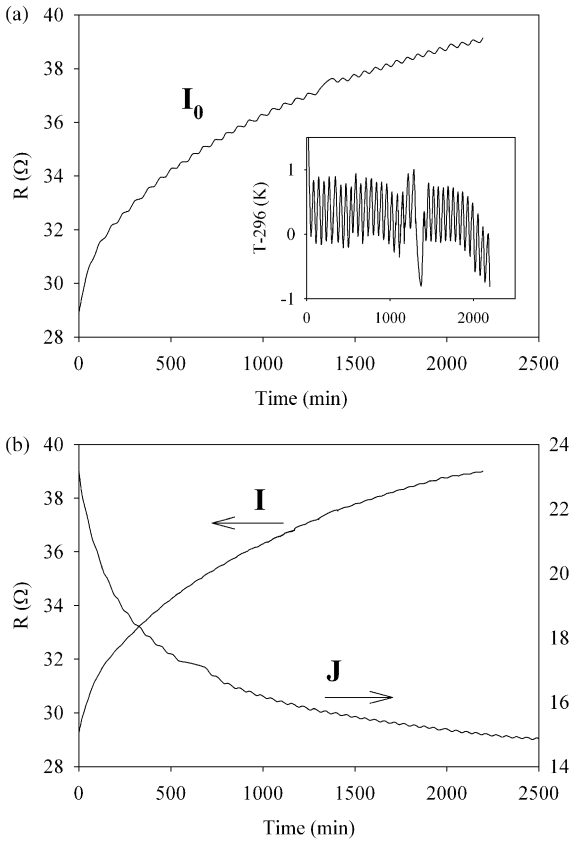

Fig. 4. The resistance of Cs_8Sn_{44} versus time at room temperature. (a) raw data for the sample status I, inset of (a): the room temperature versus time. (b) Curve I: resistance at 296 K corrected with the room temperature fluctuation. Curve J: corrected resistance for sample status J.

In our experiments, we observed prominent relaxation effect for R right after change of pressure. Fig. 4(a) shows the room temperature resistance measured as a function of time at 0.60 GPa with the following: the sample was first pressurized to 1.20 GPa (E), then the pressure was reduced to 0.15 GPa (G), relaxed for 3 days (H) then increased to 0.60 GPa (I). It showed an exponential relaxation effect with some periodic fluctuations. A plot of the temperature versus temperature (inset of Fig. 4(a)) showed that this effect is due to the small temperature fluctuation in the air-conditioned laboratory, so we label this raw curve as I_0. Curve I in Fig. 4(b) shows the corrected resistance at $T = 296$ K, with a fitted value $dR/dT = -0.164 \pm 0.002$ Ω/K. Curve J is the corrected resistance at $T = 296$ K with a fitted value $dR/dT = +0.012 \pm 0.001$ Ω/K for sample reduced from 0.60 (I) to 0 GPa. Apparently the correction for curve J is not as good as curve I. Nevertheless, we noticed that the sign changed again for dR/dT around room temperature after the pressure is dropped. A simple Arrhenius law does not give perfect fit for these two curves, while the fit based on 1-D bulk diffusion with a delta function as initial condition is perfect [24]

$$\frac{R(t) - R(0)}{R(\infty) - R(0)} = 1 - \frac{8}{\pi^2}\sum_{m=0}^{\infty}\frac{1}{(2m+1)^2}\exp\left[\frac{-(2m+1)t^2}{\tau}\right]. \quad (3)$$

Using the first four terms and τ as the only adjustable parameter, curve I can be fit by $\tau = 1295 \pm 3$ min and curve J can be fit by $\tau = 1076 \pm 4$ min.

The relaxation effect of resistivity might be affected by some extrinsic conditions, e.g. grain boundaries. We ruled out this possibility based on two facts. One fact is that the value of R increases with increasing pressure by a factor of about two, which is larger than what would be expected from grain boundary effects. Additionally, the change of the value is opposite to what would be caused by improvement of grain boundaries.

After long enough relaxation (~3 days at room temperature), the resistivity was essentially reversible, with a small residual decrease likely due to the improvement of grain boundaries, as mentioned earlier. Furthermore, if we compare the resistance before and after relaxation in logarithm scale (Fig. 5), we can see that the two curves are

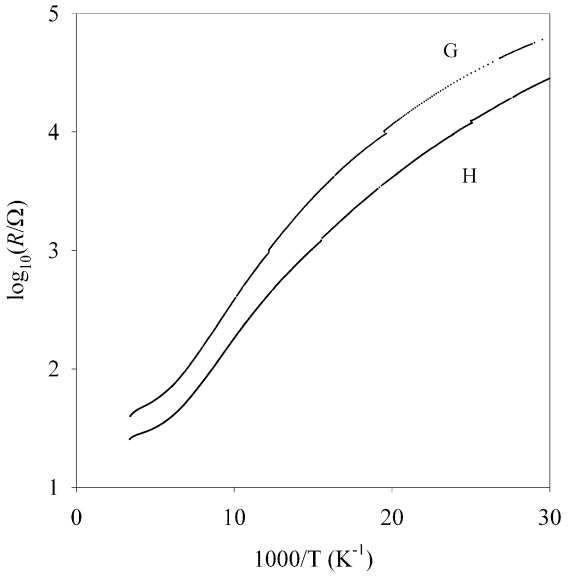

Fig. 5. The resistance of Cs_8Sn_{44} at pressure reduced from 1.20 to 0.15 GPa before (G) and after (H) relaxation at room temperature for 3 days.

remarkably parallel, indicating that E_1 and E_2 did not change during the phase of relaxation.

Other pressure experiments [25] show that under high pressure, the carriers may move from one location to another location, introducing a relaxation effect. Cs_8Sn_{44} has two vacancy sites per unit cell, and the relaxation effect caused by increasing pressure might be directly linked to a vacancy change. Our experiment indicates that the pressure changed both the band gap(s) and vacancy, the previous one is an immediate effect, while the vacancy change might take very long to be fully relaxed.

We did not observe the relaxation effect in S within our experimental resolution. Thus this null result is a strong indication that the Seebeck coefficient is directly related to the energy gap of Cs_8Sn_{44}. This would further indicate that the Seebeck coefficient is only affected by the electronic structures, which was not affected by the finely distributed vacancies, while the resistivity was affected by both.

One of the most important results of this set of experiments is the irreversible effect on S under high pressure. The pressure was applied to the sample in steps, first increasing the pressure from ambient pressure (A) to 0.30 GPa (B), 0.60 GPa (C), 0.90 GPa (D), 1.20 GPa (E), then decreasing to 0.45 GPa (F) and 0.15 GPa (G), and finally allowing the sample to relax room temperature for 3 days (H). The Seebeck coefficient increases with increasing pressure and is not reversible; the Seebeck coefficient remains higher. To further verify this, we measured the Seebeck coefficient inside the pressure cell at ambient pressure and then take the sample out, waited a week at room temperature, then remeasured S. Both values at room temperature are -342 ± 2 μV/K. Thus the irreversible effect on Seebeck coefficient is induced by pressure and has no observable relaxation.

Bundy et al. observed transition towards metallic phase at pressure of 11 GPa for clathrate Na_3Si_{34} and at higher pressure for $Na_{11}Si_{34}$ [9]. San-Miguel et al. observed structural transformation to β-Sn structure under high pressure for clathrate Si_{34} at 11.0 GPa [10]. Meng et al. reported room temperature thermopower measurement of Ge-based clathrate $Sr8Ga_{16}Ge_{30}$ under quasi-hydrostatic pressure [13]. They did not observe any structural changes up to 7.5 GPa. Our maximum pressure is only 1.2 GPa and is much lower than that of a drastic structural transformation may probably occur. The complicated effects we observed here should be introduced by other factors.

Cs_8Sn_{44} is know to have the type-I clathrate structure. The Sn atoms form the characteristic host cage with Cs atoms as guests, 'rattling' in the center. Typically for type-I clathrate, three crystallographic sites are named 6c, 16i and 24k sites, respectively [14,16]. Nolas et al. [16] have shown that the two intrinsic vacancies for Cs_8Sn_{44} are at 6c site. However, the actual distribution of the vacancies on the 6c sites were not determined. It is reasonable to assume the vacancy sites are randomly distributed in 6c sites. However, Dong et al. [15] have shown from band structure calculations there are two favorable configurations for local energy minimum, namely, placing the two vacancies on 6c sites that are on the same hexagonal surface or different hexagonal surfaces. Under high pressure, it is possible that the vacancy changes from one 6c site to another site. This would account for the irreversible change of S under high pressure. Furthermore, the relaxation effect observed in R measurement can also be attributed to some direct effect of vacancy fluctuation or relocation.

More interestingly, Dong's calculation showed that there are two nearly degenerate conduction bottoms which have two different pressure dependence. These two band gaps cross to each other near the pressure of 1 GPa. This pressure coincides with the value at which further increase of pressure reduced the absolute value of the Seebeck coefficient of Cs_8Sn_{44}. However, we are not able to explain the fine features of our experiments by the theory satisfactorily yet.

It would be nice if we could conduct a comparison experiment on Cs_8Sn_{46} which does not have any vacancies. However, such a material is not available to date. Probably this kind of 'perfect' structure is not stable. An alternative is $Cs_8Zn_4Sn_{42}$ [14]. The structures of both Cs_8Sn_{44} and $Cs_8Zn_4Sn_{42}$ can be written as $Cs_8A_nSn_{46-n}$. For Cs_8Sn_{44}, A is vacancy and $n = 2$; while for $Cs_8Zn_4Sn_{42}$, A is Zn and $n = 4$. However, the numbers of defects per unit cell are different for these two materials and the nature of the defects is also different. Nevertheless, we conducted the resistivity and Seebeck coefficient measurements on $Cs_8Zn_4Sn_{42}$ under high pressure for comparison.

Our experiments show that the relaxation effect of R for $Cs_8Zn_4Sn_{42}$ is $\leq 2\%$, which is 1–2 orders smaller than that of

Cs_8Sn_{44}. This can be understood considering that it is much more difficult to move Zn atoms from one Sn site to another in $Cs_8Zn_4Sn_{42}$ than it is to move vacancies around in Cs_8Sn_{44}. However, an increase in the magnitude of the Seebeck coefficient with pressure is observed for $Cs_8Zn_4Sn_{42}$. Further, this increase is not reversible either (after application of high pressure) as in Cs_8Sn_{44}. On the other hand, the Seebeck coefficient is fully reversible after application of high pressure for systems like Bi_2S_3 [26]. The cause of the irreversible change in Seebeck coefficient for Sn clathrates is currently under investigation.

5. Conclusions

We have measured the resistivity and Seebeck coefficient of Cs_8Sn_{44} and $Cs_8Zn_4Sn_{42}$ as function of both hydrostatic pressure and temperature. For Cs_8Sn_{44}, two energy gaps can be distinguished from the resistivity vs. temperature data. Both the energy gap E_1 near room temperature and the energy gap E_2 for intermediate temperatures increase with increasing pressure. Compared with $Cs_8Zn_4Sn_{42}$, the prominent relaxation effect of R under high pressure is unique for Cs_8Sn_{44}, suggesting that the effect is caused by the intrinsic vacancies in Cs_8Sn_{44}. An irreversible increase in the S was observed in both Cs_8Sn_{44} and $Cs_8Zn_4Sn_{42}$ after application of pressure. We also demonstrated that the power factor can be increased permanently by application of high pressure, suggesting that a thermoelectric device with higher efficiency under high pressure is possible for real applications.

Acknowledgements

This work is supported by research grant DAAD19-99-1-0001 from the Army Research Office.

References

[1] L. Gao, Y.Y. Xue, F. Chen, Q. Xiong, R.L. Meng, D. Ramirez, C.W. Chu, J.H. Eggert, H.K. Mao, Phys. Rev. B 50 (1994) 4260.
[2] J.S. Schilling, J. Phys. Chem. Solids 59 (1998) 553–568.
[3] J.L. Cohn, G.S. Nolas, V. Fessatidis, T.H. Metcalf, G.A. Slack, Phys. Rev. Lett. 82 (1999) 779–782.
[4] G.A. Slack, Mater. Res. Soc. Symp. Proc. 478 (1997) MRS, Warrendale.
[5] G. Nolas, Mater. Res. Soc. Symp. Proc. 545 (1999) MRS, Warrendale.
[6] J.S. Tse, K. Uehara, R. Rousseau, A. Ker, C.I. Ratcliffe, M.A. White, G. MacKay, Phys. Rev. Lett. 85 (2000) 114–117.
[7] V.L. Kuznetsov, L.A. Kuznetsov, A.E. Kaliazin, D.M. Rowe, J. Appl. Phys. 87 (2000) 7871–7875.
[8] J.D. Bryan, V.I. Srdanov, G.D. Stucky, D. Schimidt, Phys. Rev. B 60 (1999) 3064–3067.
[9] F.P. Bundy, J.S. Kasper, High Temp.–High Press. 2 (1970) 429–436.
[10] A. San-Miguel, P. Kéghélian, X. Blase, P. Mélinon, A. Perez, J.P. Itié, A. Polian, E. Reny, C. Cros, M. Pouchard, Phys. Rev. Lett. 83 (1999) 5290–5293.
[11] G.K. Ramachandran, P.F. McMillan, S.K. Deb, M. Somayazulu, J. Gryko, J. Dong, O.F. Sankey, J. Phys.: Condens. Matter 12 (2000) 4013–4020.
[12] J. Dong, O.F. Sankey, G. Kern, Phys. Rev. B 60 (1999) 950–958.
[13] J.F. Meng, N.V.C. Shekar, J.V. Badding, G.S. Nolas, J. Appl. Phys. 89 (2001) 1730–1733.
[14] G.S. Nolas, J.L. Cohn, E. Nelson, Proceedings of the 18th International Conference on Thermoelectrics, IEEE Press, Baltimore, 1999.
[15] J. Dong, O.F. Sankey, C.W. Myles, unpublished.
[16] G.S. Nolas, B.C. Chakoumakos, B. Mahieu, G.J. Long, T.J.R. Weakley, Chem. Mater. 12 (2000) 1947–1953.
[17] C.W. Chu, Phys. Rev. Lett. 33 (1974) 1283.
[18] F. Chen, Z.J. Huang, R.L. Meng, Y.Y. Sun, C.W. Chu, Phys. Rev. B 48 (1993) 16,047.
[19] F. Chen, Q.M. Lin, Y.Y. Sun, C.W. Chu, Physica C 282–287 (1997) 1245–1246.
[20] F. Chen, J.C. Cooley, W.L Hults, J.L Smith, Rev. Sci. Instrum. 72 (11) (2001) 4201–4206.
[21] R.B. Roberts, Philos. Mag. 36 (1977) 91.
[22] D.K.C. MacDonalds, Thermoelectricity: An Introduction to the Principles, Wiley, New York, 1962.
[23] H.J. Goldsmid, Electric Refrigeration, H. Temple Press, London, 1986.
[24] I.S. Sokolnikoff, E.S. Sokolnikoff, Higher Mathematics for Engineers and Physicists, McGraw-Hill, New York, 1941.
[25] S. Sadewasser, J.S. Schilling, J.L. Wagner, O. Chmaissem, J.D. Jorgensen, D.G. Hinks, B. Dabrowski, Phys. Rev. B 60 (1999) 9827.
[26] F. Chen, J. Fang, K.L. Stokes, unpublished.